

# Zero gravity thermal convection in granular gases

A. Rodríguez-Rivas, M. A. López-Castaño, and F. Vega Reyes  
*Departamento de Física and Instituto de Computación Científica Avanzada (ICCAEx),  
Universidad de Extremadura, 06006 Badajoz, Spain*

(Dated: June 25, 2021)

Previous experimental and theoretical evidences have shown that convective flow may appear in granular fluids, if subjected to a thermal gradient and gravity (Rayleigh-Bénard type convection). In contrast to this, we present here evidence of gravity-free thermal convection in a granular gas, with no presence of external thermal gradients either. Convection is here maintained steady by internal gradients due to dissipation and thermal sources at the same temperature. The granular gas is composed by identical disks and is enclosed in a rectangular region. Our results are obtained by means of an event driven algorithm for inelastic hard disks.

Granular dynamics has been an interesting test ground in the last decades for non-equilibrium statistical mechanics and complex fluid mechanics [1, 2]. We know from previous works that much of the phenomenology observed in molecular gases and condensed matter [3] arises in granular matter as well, but in general with added complexity. Phenomena like jamming [4–7], crystallization [8–10], glass transitions [11, 12], capillarity [13], fluid flow and convection [14, 15], memory effects [16, 17] etc., appear also in granular matter systems. But, furthermore, there is also a rich phenomenology which is intrinsic to granular media, such as clustering instabilities in low density systems [18, 19] or inelastic collapse in denser systems [20].

Granular convection and pattern formation in systems under gravity has been known for quite some time now [1, 21, 22]. It has been observed for instance in experiments with vertically oscillated particles [23, 24]. In the case of horizontally unbounded low density systems, previous works have provided complete descriptions of the different types of patterns that can be observed by means of computer simulations [24–26] and theoretical studies [27, 28]. These works have shown the existence of a formal analogy with the classical Rayleigh-Bénard convection in molecular fluids [14]. However, experimental work shows, to a certain degree, a mismatch with the theory; for instance, in the threshold values of the buoyancy driven convection [29]. Part of the origin of this disagreement stems from the existence of another type of convection mechanism due to dissipation at the sidewalls. And of course, sidewalls are inherently present in granular dynamics experiments. In fact, the presence of sidewalls is known to have impact on hydrodynamic instabilities in general, even if they are physically inert [14, 26, 30]. More specifically, thermal convection induced by sidewall energy leaks is well known in molecular fluids [31]. For granular materials, a similar mechanism is triggered by wall-particle inelastic collisions, rather than a thermal leak [32–35].

In any case, and to our knowledge, thermal convection in granular dynamics has always been detected in the

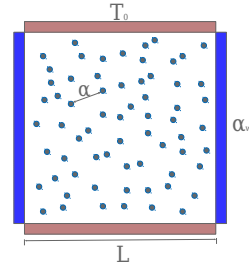


Figure 1. Sketch of the system. The only thermal sources are at the upper and bottom walls (both set at the same temperature  $T_0$ , thus injecting energy to particles nearby through a standard computational procedure [39]), and without inducing temperature difference between the fluid near both walls. The other two parallel walls (left and right) are inert and dissipative; i.e. particles undergo inelastic collisions at contact with these walls.

presence of a gravitational field (see references above and their bibliographies) [36]. We now prove the existence of zero-gravity granular thermal convection [37]. Furthermore, as we will show, the intrinsic thermal gradient (induced by particle-particle inelastic collisions [34]) is not strictly necessary to produce convection, requiring only sidewalls energy dissipation (and the presence of thermal walls, that set the steady state temperature value). This result obviously has an impact in granular matter applications under microgravity or no gravity conditions (involving mining, storage and transportation of granular matter), and in experiments in the near future by space agencies [38]. For instance, an experimental evidence of the new convection is foreseeable in the context of research projects in low-gravity or no gravity environments [22].

Let us describe our system in more detail. We deal with a 2D granular gas enclosed in a square-shaped system, as sketched in Figure 1. Particles are identical smooth hard disks with mass  $m$  and diameter  $\sigma$ , used as mass and length units in this work. Particle density  $n$  remains sufficiently low at all times in the system, so that collisions are always binary and instantaneous. Since we

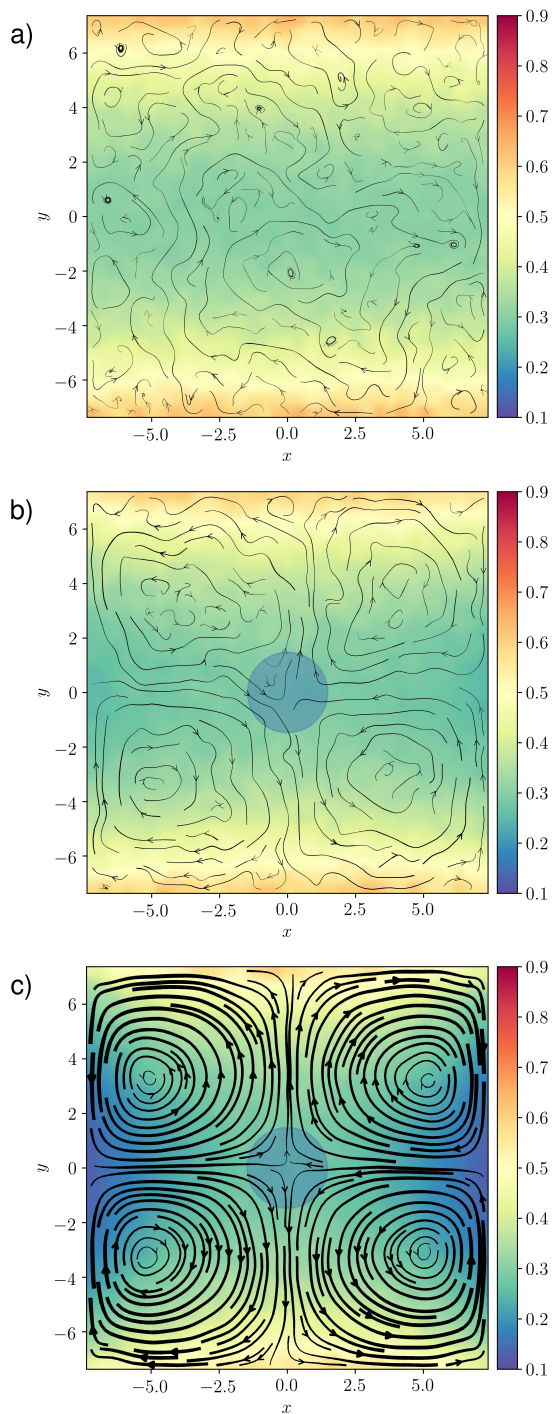


Figure 2. Flow velocity ( $\mathbf{u}$ ) and granular temperature ( $T$ ) hydrodynamic fields, with  $\alpha = 0.9$ ,  $L = 15\lambda$ , and: (a)  $\alpha_w = 1$  (elastic sidewalls, no convection), with  $u_{\max} = (\sqrt{u_x^2 + u_y^2})_{\max} = 0.00272$ ; (b)  $\alpha_w = 0.9$  (incipient convection), with  $u_{\max} = 0.00363$ ; (c)  $\alpha_w = 0.6$  (fully developed convection), with  $u_{\max} = 0.04008$ . Line thickness is relative to flow intensity. Flow centers appear highlighted in clear blue.

use the smooth hard particle collisional model, rotational

degrees of freedom are neglected [27]. Coefficients of normal restitution  $\alpha$  and  $\alpha_w$  characterize the degree of inelasticity upon particle-particle and sidewall-particle collisions respectively [34]. A pair of thermal walls injects kinetic energy to nearby particles. We label the other two walls as 'lateral' walls or sidewalls. The system is free of any gravitational field, thus avoiding any possibility of buoyancy driven convection.

As seen in a previous work [34], if a system like the one in Figure 1 is under the action of gravity, there is no mathematical solution to the corresponding hydrodynamic equations for a hydrostatic state,  $\mathbf{u} = \mathbf{0}$ . Therefore, the action of gravity combined with dissipative sidewalls leads automatically to convection (this happens in molecular fluids as well [31]). But this is not so in the absence of gravity.

In effect, by taking into account the symmetry properties for the system in the steady state ( $\partial/\partial t = 0$ ), we can obtain the corresponding equations for a hydrostatic state [39] by imposing the condition  $\mathbf{u} = \mathbf{0}$  on the granular gas balance equations. For disks we obtain the following differential equation for the temperature [15]

$$\frac{\sqrt{T}}{\pi\sigma^2} \left[ \frac{\partial}{\partial x} \left( \sqrt{T} \frac{\partial T}{\partial x} \right) + \frac{\partial}{\partial y} \left( \sqrt{T} \frac{\partial T}{\partial y} \right) \right] = \frac{\zeta^*(\alpha)}{\kappa^*(\alpha)} p^2, \quad (1)$$

which now admit a non-trivial solution. Hence, the base state (the simplest hydrodynamic state) for  $g = 0$  is a hydrostatic one. In (1),  $p$  is the hydrostatic pressure,  $T$  is the granular temperature,  $\kappa^*(\alpha)$  is the transport coefficient associated to the heat flux and  $\zeta^*(\alpha)$  is the cooling rate due to particle-particle inelastic collisions [40]. This means that an eventual gravity-free convection would appear only under certain conditions.

In order to analyze the problem, we perform event driven simulations of inelastic smooth hard disks [39, 41]. Throughout this work, results are represented in dimensionless variables (denoted with the same symbols as their dimensional counterparts), by using  $\sigma$ ,  $\tau = \sqrt{m\sigma^2/T_0}$ ,  $m$  and  $T_0$  as units of length, time, mass and temperature, respectively; where  $T_0$  is the thermal walls temperature. In order to characterize particle density, we use the two-dimensional packing fraction  $\bar{\phi} = N\pi\sigma^2/4L^2 = 10^{-3}$ , being  $N$  the total number of disks in the system. Therefore the mean free path is  $\lambda = (2\sqrt{\pi\bar{n}\sigma})^{-1} = 221.5567$ , where  $\bar{n} = N/L^2$  is the system average particle density. The specifics of the simulation are discussed in the Supplemental Material file [39].

Figure 2 displays flow velocity ( $\mathbf{u}$ ) and granular temperature ( $T$ ) fields for a system with  $L = 15\lambda$  and  $\alpha = 0.9$ , for three different  $\alpha_w$  values ( $\alpha_w = 1, 0.9$  and  $0.6$ ). As it can be seen, convection is initially absent for  $\alpha_w = 1$  (only remnant noise is observed) but develops for  $\alpha_w \leq \alpha_w^{\text{th}}(\alpha) < 1$ , where  $\alpha_w^{\text{th}}(\alpha)$  is the convection critical

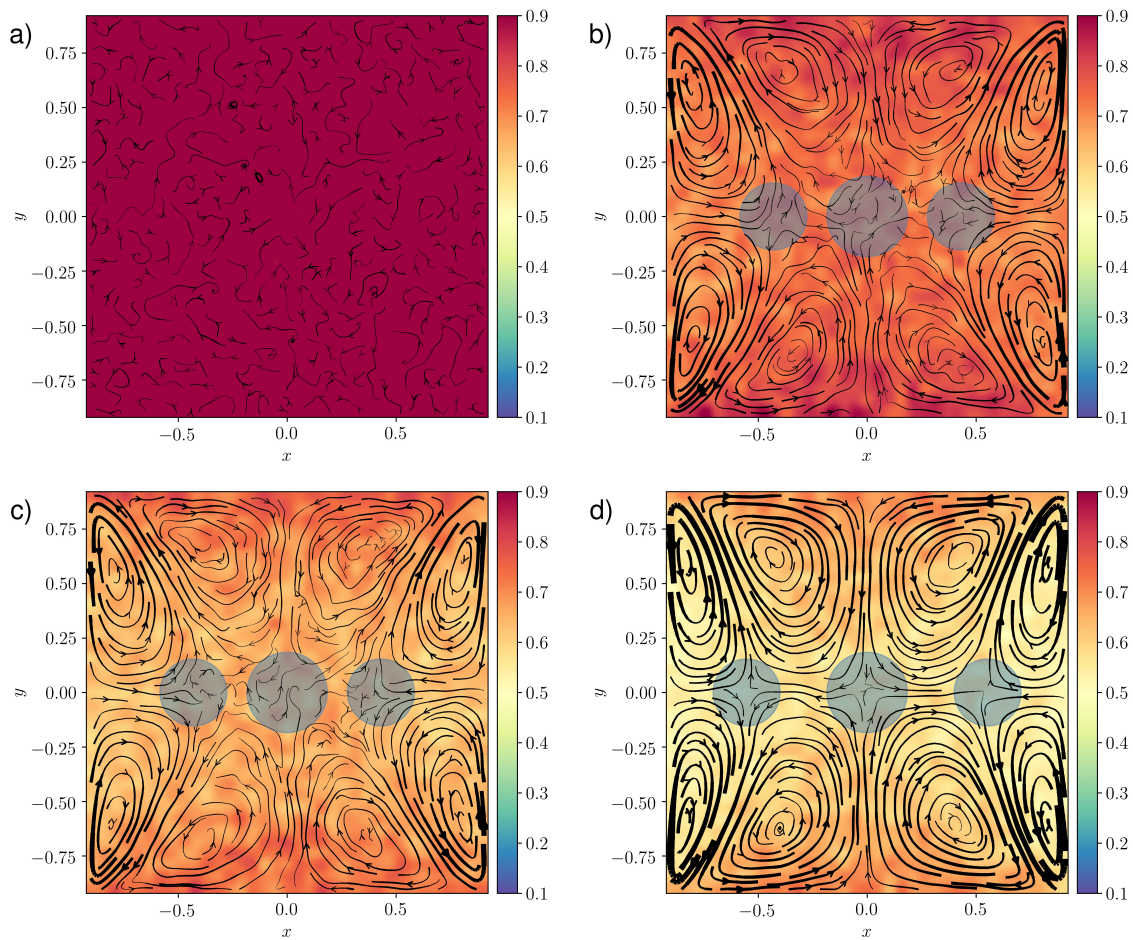


Figure 3. Hydrodynamic fields  $\mathbf{u}$  and  $T$  for  $L = (15/8)\lambda$ , with: (a)  $\alpha = 1.0$ ,  $\alpha_w = 1.0$ ;  $u_{\max} = 0.00450$ , (b)  $\alpha = 1.0$ ,  $\alpha_w = 0.7$ ;  $u_{\max} = 0.02453$ , (c)  $\alpha = 0.9$ ,  $\alpha_w = 0.7$ ;  $u_{\max} = 0.02254$ , (d)  $\alpha = 0.9$ ,  $\alpha_w = 0.5$ ;  $u_{\max} = 0.03686$ . Flow centers appear highlighted in clear blue.

value, that depends on  $\alpha$  and the other system parameters. Moreover, convection is strongly dependent on the parameter  $\alpha_w$ , this being possibly due to the strong correlation between sidewalls dissipation and the temperature gradient [39]. Notice that, in the presence of gravity, sidewall dissipation generates just one cell attached to each dissipative wall [34], whereas now we find 2 convective cells per dissipative wall. This result makes sense since, for our geometry and with  $g = 0$ , streamlines should have two perpendicular axes of specular symmetry, both passing through the center of the system.

Streamlines coming from dissipative sidewalls flow towards the center, then bending off the center onto the thermal walls. In fact, the orientation of the flow in the convection cells can be explained by looking at the behaviour in certain singular points, where streamlines in convection rolls meet. We mark these *flow centers* with circles in Figures 2 and 3. In this sense, we can see that in Figure 2 there is only one flow center, which coincides with the center of the system whereas in Figure 3, we find

3 flow centers: one in the system center and other two closer (and at the same distance) to the sidewalls. Notice also that these two flow centers approach the sidewalls as they become more inelastic (Figures 3c and 3d), which can be an indication that the convection mechanism is related to the inability of colder particles to reach the system center, as they flow from the sidewalls.

In Figure 3 we show the results for a smaller system ( $L = (15/8)\lambda$ ). As we see, the convection pattern is now very different. We now observe 4 cells next to dissipative walls plus 4 additional cells emerging near the system center, totalling 8 convection cells and three flow centers. Also notice that decreasing the value of  $\alpha_w$  expands the area of the four central cells while decreasing the size of the cells next to the lateral walls. A reason for the appearance of the new central cells may be that the center is now hotter than in the bigger system in Figure 2 [15]. This produces a new convection center from which streamlines flow out.

It is very important to notice (Figure 3b) that con-

vection can appear even for elastic particle-particle collisions. As we see, a 2D thermal gradient, created only by dissipation at the lateral walls ( $\alpha_w < 1$ ) and the thermal sources in the upper and lower walls is sufficient to trigger convection. Figures 2, 3 show a general trend of stronger convection for overall increasing inelasticity, this trend being more important for sidewall dissipation increase (decrease of  $\alpha_w$ ).

A convenient way to analyze the convection intensity is by looking at the vorticity field,  $\omega \equiv \partial_x u_y - \partial_y u_x$ , as in Figure 4. Two distinctive convection patterns are found, as already mentioned, with either 4 or 8 cells with alternating vorticity sign, the 4 central cells disappearing for bigger systems. Notice that, in Figure 4b, vorticity nuclei are closer to the corners. As we commented above, an important aspect of gravity-free convection is that the system allows for hydrostatic states and hence convection is not expected to appear in all cases. Figure 5 illustrates this point, where convection threshold lines are shown on the global vorticity surface  $\langle |\omega| - |\omega_0| \rangle(\alpha, \alpha_w)$ . We clearly detect non-convective (hydrostatic) regions. Moreover, the hydrostatic state tends to occupy wider regions in the parameter space as the system increases in size. Vorticity surface reveals clearly (Figure 5 b) that, although gravity-free convection is indeed stronger for more inelastic systems, the opposite trend is observed near a region close to  $\alpha_w = 0.2$ , where a significant vorticity drop towards  $\alpha_w \rightarrow 0$  is observed.

In summary, in this work we have shown the existence of gravity-free granular convection. It is produced by the existence of sufficiently strong a 2D thermal gradient out of an initially hydrostatic base state at small gradients. Since 2D thermal gradients are actually characteristic of granular experiments (usually being produced at system boundary corners), this type of convection should be present in most zero gravity experiments. From a fundamental point of view, it is interesting to remark that molecular gases should also display gravity-free convection as long as they present analogous boundaries to those studied here. In fact, analogous gravity-free natural convection may be found in liquid droplets [42, 43] due to thermocapillary effects driven by the gradients of surface tension, the difference being here that now the 2D thermal gradient is generated by the boundary curvature. From a more general point view, our results constitute a rare example of natural thermal convection with no gravity, in a generic fluid system. Moreover, it would be interesting to test if other effects such as capillarity [13] also appear under no gravity conditions. Additionally, we think the results in this work may have an impact in other contexts such as horizontal systems (common in living matter for instance). Finally, the mechanism for the onset of gravity-free natural convection is outlined.

We acknowledge funding from the Government of Spain through project No. FIS2016-76359-P and from the regional Extremadura Government through projects

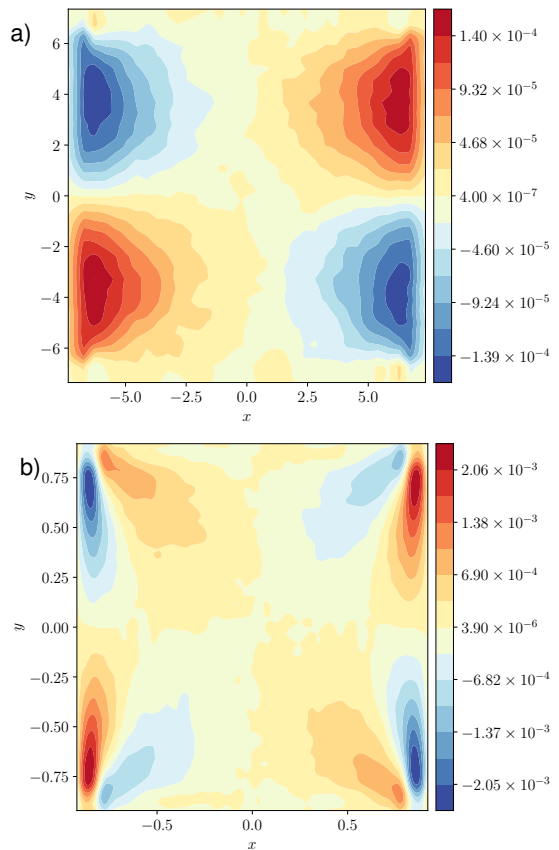


Figure 4. Vorticity field  $\omega - \omega_0$  for  $\alpha = 0.9$  and  $\alpha_w = 0.4$ , obtained for the box sizes (a) and  $L = 15\lambda$ , (b)  $L = (15/8)\lambda$ .  $\omega_0$  is the base vorticity level coming from noisy data at  $\alpha = \alpha_w = 1$ .

No. GR18079 & IB16087, both partially funded by the ERDF.

- 
- [1] H. Jaegger, S. Nagel, and R. P. Behringer, “The physics of granular materials,” *Physics Today* **49**, 32 (1996).
  - [2] I. S. Aranson and L. S. Tsimring, “Patterns and collective behavior in granular media: Theoretical concepts,” *Rev. Mod. Phys.* **78**, 641 (2006).
  - [3] P. G. de Gennes, “Soft matter,” *Rev. Mod. Phys.* **64**, 645 (1992).
  - [4] G. Parisi S. Franz, T. Maimbourg and A. Scardicchio, “Impact of jamming criticality on low-temperature anomalies in structural glasses,” *Proc. Natl. Acad. Sci. U.S.A.* **116**, 13773 (2019).
  - [5] A. J. Liu and S. R. Nagel, “Jamming is not just cool anymore,” *Nature* **396**, 21 (1998).
  - [6] K. Lu, E. E. Brodsky, and H. P. Kavehpour, “A thermodynamic unification of jamming,” *Nat. Phys.* **4**, 404 (2008).
  - [7] E. J. Banigan, M. K. Illich, D. J. Stace-Naughton, and D. A. Egolf, “The chaotic dynamics of jamming,” *Nat. Phys.* **9**, 288 (2013).

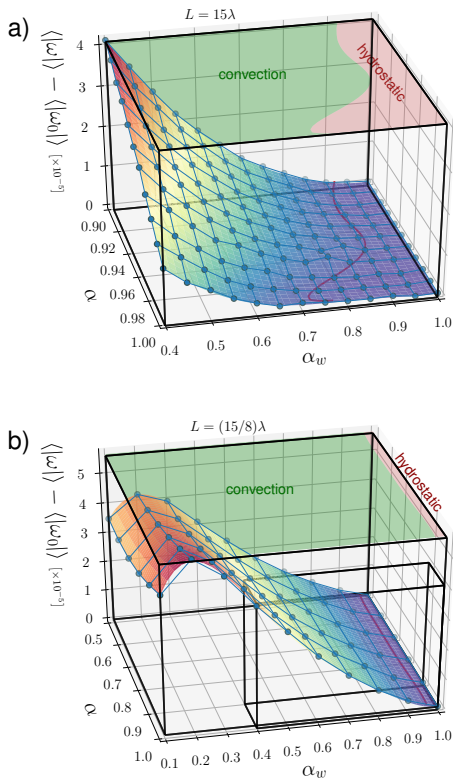


Figure 5. Global average (i.e., averaged over all points in the system) of the vorticity absolute value,  $\langle |\omega| \rangle - \langle |\omega_0| \rangle$  against  $\alpha$  and  $\alpha_w$ . (a) For  $L = 15\lambda$  and (b) For  $L = (15/8)\lambda$ . A diagram showing areas where convection/hydrostatic states is projected on the top of each figure. The curve separating both regions marks the  $\alpha_w^{\text{th}}(\alpha)$  critical values. The smaller framing box in (b) marks the parameter space represented in (a).  $\langle |\omega_0| \rangle$  is the average base vorticity absolute value coming from noisy data at  $\alpha = \alpha_w = 1$ .

[8] B. J. Alder and T. E. Wainwright, “Phase transition in elastic disks,” *Phys. Rev.* **127**, 359 (1962).  
 [9] P. Pieranski, L. Strzelecki, and B. Pansu, “Thin colloidal crystals,” *Phys. Rev. Lett.* **50**, 900 (1983).  
 [10] M. Schmidt and H. Löwen, “Freezing between two and three dimensions localized,” *Phys. Rev. Lett.* **76**, 4552 (1996).  
 [11] W. Kob and H.C. Andersen, “Scaling behavior in the  $\beta$ -relaxation regime of a supercooled lennard-jones mixture,” *Phys. Rev. Lett.* **73**, 1376 (1994).  
 [12] J. Plagge and C. Heussinger, “Melting a granular glass by cooling,” *Phys. Rev. Lett.* **110**, 078001 (2013).  
 [13] Fengxian Fan, Eric J.R. Parteli, and Thorsten Pöschel, “Origin of Granular Capillarity Revealed by Particle-Based Simulations,” *Phys. Rev. Lett.* **118**, 218001 (2017).  
 [14] M. Cross and P. C. Hohenberg, “Pattern formation outside of equilibrium,” *Rev. Mod. Phys.* **65**, 851 (1993).  
 [15] F. Vega Reyes and J. S. Urbach, “Steady base states for navier–stokes granular hydrodynamics with boundary heating and shear,” *J. Fluid Mech.* **636**, 267–293 (2009).  
 [16] A. J. Kovacs, J. J. Aklonis, J. M. Hutchinson, and A. R. Ramos, “Isobaric volume and enthalpy recovery

of glasses. II. A transparent multiparameter theory,” *J. Polym. Sci. Pt. B-Polym. Phys.* **17**, 1097–1162 (1979).  
 [17] A. Lasanta, F. Vega Reyes, A. Prados, and A. Santos, “On the emergence of large and complex memory effects in nonequilibrium fluids,” *New. J. Phys.* **21**, 033042 (2019).  
 [18] I. Goldhirsch and G. Zanetti, “Clustering instability in dissipative gases,” *Phys. Rev. Lett.* **70**, 1619 (1993).  
 [19] C. C. Maaß, N. Isert, G. Maret, and C. M. Aegerter, “Experimental investigation of the freely cooling granular gas,” *Phys. Rev. Lett.* **100**, 248001 (2008).  
 [20] J. S. Olafsen and J. S. Urbach, “Clustering, order and collapse in a driven granular monolayer,” *Phys. Rev. Lett.* **81**, 4369–4372 (1998).  
 [21] M. Faraday, “On a peculiar class of acoustical figures; and on certain forms assumed by groups of particles upon vibrating elastic surfaces,” *Phil. Trans. R. Soc. Lond.* **121**, 299 (1831).  
 [22] S. Aumaître, R. P. Behringer, A. Cazaubiel, E. Clément, J. Crassous, D. J. Durian, E. Falcon, S. Fauve, D. Fischer, A. Garcimartín, Y. Garrabos, M. Hou, X. Jia, C. Lecoutre, S. Luding, D. Maza, M. Noirhomme, E. Opsomer, F. Palencia, T. Pöschel, J. Schöckmel, M. Sperl, R. Stannarius, N. Vandewalle, , and P. Yu, “An instrument for studying granular media in low-gravity environment,” *Rev. Sci. Instrum.* **89**, 075103 (2018).  
 [23] P. B. Umbanhowar, F. Melo, and H. L. Swinney, “Localized excitations in a vertically vibrated granular layer,” *Nature* **382**, 793 (1996).  
 [24] C. Bizon, M. D. Shattuck, J. B. Swift, W. D. McCormick, and H. L. Swinney, “Patterns in 3d vertically oscillated granular layers: Simulation and experiment,” *Phys. Rev. Lett.* **80**, 57 (1998).  
 [25] C. Bizon, M. D. Shattuck, J. R. de Bruyn J. B. Swift, W. D. McCormick, and H. L. Swinney, “Convection and diffusion in patterns in oscillated granular media,” *J. Stat. Phys.* **93**, 449 (1998).  
 [26] R. Ramírez, D. Risso, and P. Cordero, “Thermal convection in fluidized granular systems,” *Phys. Rev. Lett.* **85**, 1230 (1998).  
 [27] E. Khain and B. Meerson, “Onset of thermal convection in a horizontal layer of granular gas,” *Phys. Rev. E* **67**, 021306 (2003).  
 [28] P. R. Nott, M. Alam, K. Agrawal, R. Jackson, and S. Sundaresan, “The effect of boundaries on the plane couette flow of granular materials: a bifurcation analysis,” *J. Fluid Mech.* **397**, 203 (1999).  
 [29] P. Eshuis, K. van der Weele, D. van der Meer, R. Bos, and D. Lohse, “Phase diagram of vertically shaken granular matter,” *Phys. Fluids* **19**, 123301 (2007).  
 [30] A. T. Pérez, P. A. Vázquez, J. Wu, and P. Traoré, “Electrohydrodynamic linear stability analysis of dielectric liquids subjected to unipolar injection in a rectangular enclosure with rigid sidewalls,” *J. Fluid Mech.* **758**, 586 (2014).  
 [31] P. Hall and I. C. Walton, “The smooth transition to a convective regime in a two-dimensional box,” *Proc. B. Soc. Lond. A* **358**, 199 (1977).  
 [32] R. Wildman, J. Huntley, and D. Parker, “Convection in highly fluidized three-dimensional granular beds,” *Phys. Rev. Lett.* **86**, 3304 (2001).  
 [33] J. Talbot and P. Viot, “Wall-enhanced convection in vibrofluidized granular systems,” *Phys. Rev. Lett.* **89**, 064301 (2002).

- [34] G. Pontuale, A. Gnoli, F. Vega Reyes, and A. Puglisi, “Thermal convection in granular gases with dissipative lateral walls,” *Phys. Rev. Lett.* **117**, 098006 (2016).
- [35] C. R. K. Windows-Yule, E. Lanchester, D. Madkins, and D. J. Parker, “New insight into pseudo-thermal convection in vibrofluidised granular systems,” *Sci. Rep.* **8**, 12859 (2018).
- [36] We know only of one case of granular gas convection with no gravity reported in the recent 2018 work by Windows-Yule et al. (see their reference in the bibliography), but in that case convection is generated by a ratchet effect, and therefore is not strictly a case of thermal convection.
- [37] As noted in the reference by Aumaître et al. in our bibliography, even under low-gravity, convection has been detected just in a computational study with polydisperse granular materials, but not under strictly zero-gravity conditions.
- [38] T. Steinpilz *et al.*, “ARISE: A granular matter experiment on the international space station,” *Rev. Sci. Instr.* **90**, 104503 (2019).
- [39] See Supplemental Material for details.
- [40] J. J. Brey and D. Cubero, “Granular gases,” (Springer-Verlag, Berlin, 2001) Chap. Hydrodynamic transport coefficients of granular gases, pp. 59–78.
- [41] Syed Rashid Ahmad and Sanjay Puri, “Velocity distributions and aging in a cooling granular gas,” *Phys. Rev. E* **75**, 031302 (2007).
- [42] H. Kim, K. Muller, O. Shardt, S. Afkhami, and H. A. Stone, “Solutal Marangoni flows of miscible liquids drive transport without surface contamination,” *Nature Phys.* **13**, 1105 (2017).
- [43] J. Park, H. J. Sung, and H. Kim, “Bulletin of the American Physical Society, 71st Annual Meeting of the APS DFD. Controlling flow patterns inside a sessile droplet using external volatile liquid,” (2018) p. 620.